Surface & Coatings Technology 205 (2011) 4073–4078

Contents lists available at ScienceDirect

Surface & Coatings Technology

journal homepage: www.elsevier.com/locate/surfcoat

Breakdown characteristics of titanium dioxide–silicone–fluorophlogopite nanocomposite coating

Yakui Bai [a], Yunhan Ling [b,*], Xinde Bai [b]

[a] College of Nuclear Science and Technology, Beijing Normal University, Beijing, 100875 China
[b] Department of Materials Science and Engineering, Tsinghua University, Beijing, 100084 China

ARTICLE INFO

Article history:
Received 25 November 2010
Accepted in revised form 22 February 2011
Available online 26 February 2011

Keywords:
Flashover
Polymers
Photoconductivity
Titanium compounds

ABSTRACT

In order to improve the high-voltage performance of organic insulators against flashover breakdown, a novel composite coating capable of conductive manipulation by the introduction of suitable amount of titanium dioxide photocatalytic semiconductor was proposed. This composite coating containing organic silicon, titanium dioxide and fluorophlogopite was fabricated on polyamide substrate by the brushing method. X-ray diffraction (XRD), scanning electron microscopy (SEM), Fourier-transform infrared spectra (FT-IR) and impedance analysis were employed to characterize the coating. Experimental results show that the composite with a very low dielectric loss at high frequencies was well-dispersed and adhered to organic substrate. A nanosecond pulse vacuum flashover test revealed that the insulation strength of nanocomposite coating had a 31.85% increase compared with standard polyamide, implying that a new mechanism could govern the electrical properties of the composite insulator adjusted by the photoconductivity of nano titanium dioxide, in which the mitigation of electron accumulation improves the rate of anti-flashover.

1. Introduction

Conducting polymers have received much attention during the past decades not only from the vantage of fundamental scientific research, but also from that of applied scientific functions. Polyamide 1010 is a common engineering plastic. Its molecular structure is a long carbon chain [1]. It evinces several advantages such as wear-resistance, insulativity, and corrosion resistance [2], and therefore has a wide application in various fields in the machinery, chemical, and military industry.

When pertaining to high voltage electrical equipment, nylon is used as a common insulation supporting material in vacuum-insulated dielectrics. However, the resistance capacity of nylon to high voltage is greatly reduced because of the surface flashover phenomenon, where electric breakdown happens on a vacuum-nylon surface interface. Many methods, such as changing the geometry [3], altering the surface conditions [4], and applying materials with a low dielectric constant [5], were already employed to improve the insulation capacity of support materials in vacuum-insulated dielectrics.

For electrical insulation, composite insulators filled with mica are widely used because of their high-voltage resistance. As an insulation material, fluorophlogopite offers better insulation and is more chemically pure than natural mica [6].

Titanium dioxide is currently attracting much interest for its semiconductor properties. This compound has been widely used as a photo-produced semiconductor. Titanium dioxide has three crystal forms: anatase, rutile, and brookite. Anatase titanium dioxide exhibits semiconductor properties under ultraviolet and visible light radiation. Titanium dioxide has the advantages of high chemical stability, high photo catalytic activity to oxidize pollutants in air and water, relative low-price, and nontoxicity [11–14].

Most polymeric materials are usually dielectrics, and many of them are good insulators. Methods like dip coating in solution, ion implantation [18,19] etc. have been employed to alter the polymer properties so that the material becomes conducting. A number of earlier studies [20,21] have established that nanoparticle-semiconductor doping increases conductivity of the polymers; but specific changes in the polymer in relation to an increase in conductivity and the mechanisms of conduction are far from being well understood.

With its unique interface, small size, quantum size and macroscopic quantum tunneling effects, nano-inorganic particles show many new features in nanocomposite material. In recent years, nano-inorganic particles achieved popularity for modifying polymers by improving the mechanical, optical, thermal and other properties of composite materials. However, only few reports have been published on nanomaterials used in improving their insulating properties in an electric field.

The aim of our study is to monitor the changes in the electrical properties of the insulator polyamide 1010 after being coated by nano particles and to obtain the most suitable dosage by comparing electrical properties with those produced by different nanoparticles.

* Corresponding author. Tel.: +86 10 62772856; fax: +86 10 62772507.
E-mail address: yhling@mail.tsinghua.edu.cn (Y. Ling).

0257-8972/$ – see front matter © 2011 Elsevier B.V. All rights reserved.
doi:10.1016/j.surfcoat.2011.02.055

2. Theoretical background

Much work has been conducted with secondary electron emission from polymeric insulators [22–24] and this attention continues nowadays because of its important applications in fields like insulator breakdown (maybe damaging electronic devices). To maintain a high voltage against breakdown under vacuum conditions, both insulators and insulation coatings (or composite insulator material by doping) are used. Often, this is an environment where free charges abound. Hence, the insulators are bombarded by these charges. This leads two effects: 1) new charges (secondary electrons) are created and ejected into the ambient vacuum. Hence, there appears a secondary electrons emission in the triple conjunction point on the surface of an insulator [25]; and 2) the surface of the insulator gains charge, thus modifying the potential distribution [26]. Because of its relevance to the practical problem of voltage hold-off, the emission of secondary electrons is continually being studied in specific experiments [27].

Surface discharge of polymeric materials is the crucial point against insulation breakdown in engineering applications. The surface discharge characteristics are determined not only by the structure of polymeric materials, but also by temperature, humidity, and pressure in the application environment.

Secondary electron emission processes in nanosecond pulse under vacuum play an essential role in vacuum electronic devices. Materials used in the devices may need to be carefully scrutinized and selected to enhance and, in some cases, to suppress the secondary electron emission [28]. In microwave and millimeter wave power tubes, low secondary electron emission materials are desirable for depressed collectors in order to ensure high efficiency in the energy conversion [29,30]. Low secondary electron emission materials are also sought for coating the grids and the tube walls to prevent RF vacuum breakdown [7,8]; more evidences show that surface modification via nano coating might be a new alternative.

3. Experimental

3.1. Materials

Bulk polyamide 1010 (PA1010) was purchased from Shanghai cellulose factory. Titanium dioxide nano powder (average size 30 nm) is provided by Nanjing Haitai Nano Co. and organic silicone resin with 50% silicone content was provided by Chenguang Chemical Plant (China).

Bulk PA l010 and titanium dioxide nano-powder were desiccated at 120 °C for 10 h in a drying furnace.

3.2. Fabrication of composite sample

3.2.1. Synthesis of nano TiO_2-organic silica sol

Solvent-ultrasonic dispersion was used to prepare the surface composite samples. A percentage of dehydrated nano TiO_2 particles and fluorophlogopite was added to a quantity of ethanol with magnetic stirring. The hybrids were processed repeatedly with ultrasonic treatment to remove the adsorbed gases contained within the nanopowders. Silicone glass resin was added to disperse the system with stirring after spilling off the upper ethanol solution. The dispersed system underwent ultrasonic treatment repeatedly to disperse the nano-particles well. The nano-TiO_2-organic silica sol was prepared.

3.2.2. Synthesis of composite sample

Nylon 1010 was cut into a cylinder with a certain diameter and thickness and its surface was cleaned through sonication in deionized water. The nylon 1010 cylinder was then dehydrated in a drying oven at 120 °C for 2 h.

The nano-dispersed resin was brushed on the surface of nylon 1010 cylinder, the thickness of the composite coating was about 0.25 mm. Composite sample was finally obtained after 12 h of vacuum-drying at 60°.

3.3. Characterization of nanocomposite coating on sample

Fourier-transform infrared spectra (FT-IR), X-ray diffraction (XRD), high-frequency impedance analysis and scanning electron microscopy (SEM) were employed to characterize the coating.

Nanosecond pulse flashover breakdown experiment was used to investigate insulation strength of the coating in vacuum.

4. Results and discussion

4.1. Scanning electron microscopic characterization

Nanocomposites were added to the nylon 1010 cylinder surface evenly according to nanocomposite colloidal coating method. In nanocomposite colloids, the average particle size of uniformly dispersed, partially agglomerated nano-TiO_2 was between 100 nm and 500 nm. Nano-TiO_2 particles were still uniformly dispersed in the dispersing agents, and gained some stability. The Solvent–Ultrasonic Nanocomposite Gel method is an effective, ideal, and simple preparatory. The samples in this paper are all prepared by this method.

Fig. 1 was the surface coating of sample after discharge experiment. The surface of nylon 1010 was covered by a layer of nano titanium dioxide–silicone–fluorophlogopite composite-coating, with good uniformity and surface flatness (which can be seen in Fig. 1a). Examining further a high magnification SEM photograph (Fig. 1b) shows nano titanium dioxide–fluorophlogopite particles that were uniformly dispersed in the silicone resin. The particle size was slightly larger because

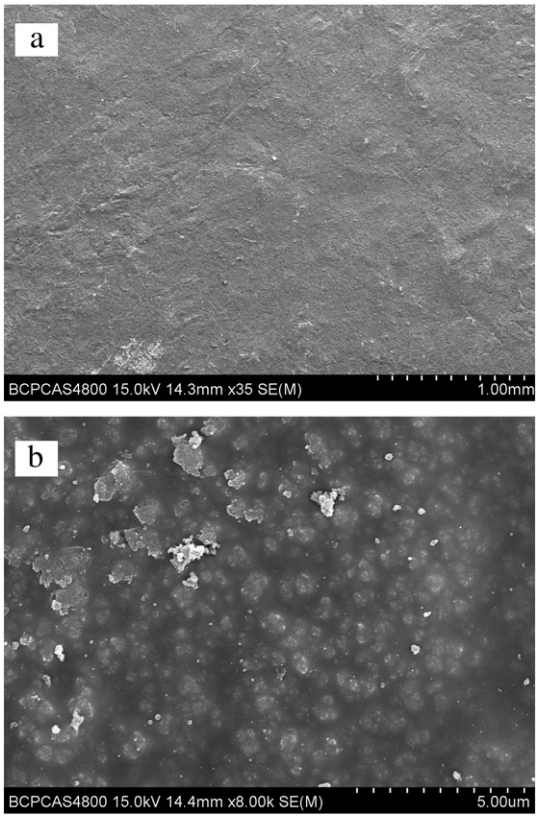

Fig. 1. SEM images of nano titanium dioxide–silicone–fluorophlogopite composite layer after nanosecond pulse vacuum flashover experiments. (a) ×35 magnification. (b) ×8000 magnification.

larger fluorophlogopite particle in composite coating were coated with nano-TiO_2 particles and formed gradually in a nanometer titanium dioxide–fluorophlogopite dispersed unit.

4.2. FT-IR analysis

Examining both Figs. 2 and 3 and the standard FT-IR vibration absorption peak of each component show that characteristic peaks of organic silicone resin were contained in an FT-IR spectrum of composite coating, in which the number and intensity of peaks were greatest. These figures indicate that the main phase in composite coating was organic silicone. The peaks in spectral regions within 3000–2500 cm^{-1} correspond to the absorption peak of C—H stretching vibration in the silicone resin; while the peaks within 1300–900 cm^{-1} correspond to the absorption peak of C – O stretching vibration in the silicone resin. In addition, peaks at 787 cm^{-1}, 651 cm^{-1} (shown in Fig. 2) and 771 cm^{-1}, and 651 cm^{-1} (shown in Fig. 3) correspond to the absorption peak of Si—O stretching vibration in the silicone resin. The characteristic peaks of nylon 1010 and fluorophlogopite were also deciphered. This was illustrated by completely wrapping the nylon cylinder with organic silicon resin, in which nano titanium dioxide and fluorophlogopite particles are dispersed uniformly. They formed a complete coating on nylon surface.

4.3. X-ray diffraction analysis

Fig. 4 shows that anatase titanium dioxide, fluorophlogopite, and silicone constituted the nanocomposite coating material according to the corresponding diffraction peak in the curve. However, standard diffraction peaks corresponding to pure nylon 1010 were not include in diffraction peaks of nanocomposite coating because the sample surface is completely covered with a coating thicker than 1 μm.

4.4. High-frequency impedance and dielectric constant test and analysis

According to the field distribution theory at the triple junction point, a lower dielectric constant can significantly improve vacuum insulation. The reason is that the dielectric constant at the triple junctions affected the distribution of the potential line. The higher dielectric constant was; the greater impact on distribution of potential line became. So the field strength at the triple junction increased and the material in which breakdown voltage in vacuum was high usually exhibited a relatively low dielectric constant. We used high-frequency impedance analysis to measure relative change in surface coating vacuum insulation properties. The equipment used on high-frequency impedance and dielectric constant test was Agilent E4991A material analyzer. As a result of the sample holder (Agilent 16453A Dielectric material fixture) limitations (thickness ≤3 mm) on sample size, we cannot directly measure high-frequency impedance and dielectric constant of the sample. We can only introduce brush coating method to make the nano-composite coatings coated on the standard substrate (glass slide). The relative change on high frequency impedance and permittivity were both measured to characterize influence of the surface composite coating on vacuum insulation. Of course, the thickness of the composite coating was the same as that on the nylon sample.

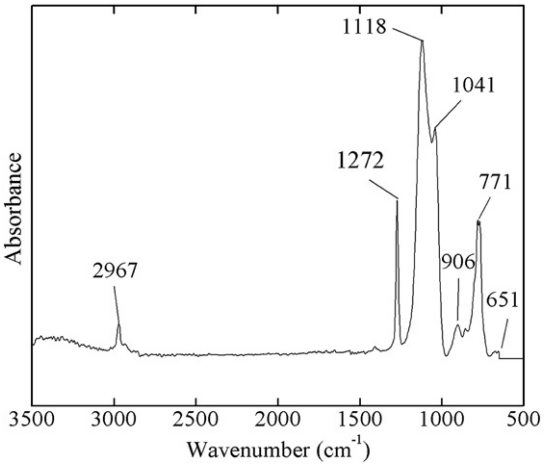

Fig. 3. FT-IR spectra of organic silicon resin.

Firstly we tested permittivity and impedance of substrate (glass slide). The dielectric constant and impedance of a binary composite coating with nano titanium dioxide, fluorophlogopite and silicone were then measured, respectively. The dielectric constant and impedance of nano titanium dioxide–silicone–fluorophlogopite ternary composite coating was finally tested. In the test, only real part of complex permittivity and impedance was recorded.

4.4.1. Permittivity measurement

According to Fig. 5, the dielectric constant of the substrate decreased significantly after silicone coating. The sample "substrate–silicone" was obtained by the nano-dispersed resin brush on the surface of substrate. The sample "substrate–mica–silicone" was obtained by the nano-dispersed resin mixed with mica brush on the surface of substrate. The sample "substrate–TiO_2–silicone" was obtained by the nano-dispersed resin mixed with nano TiO_2 brush on the surface of substrate. The total thickness of the different composite coating samples was the same.

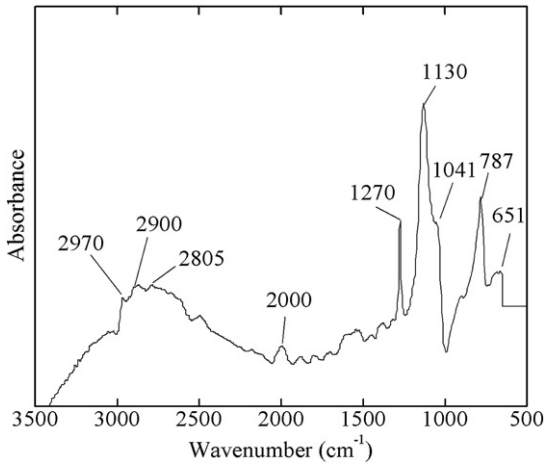

Fig. 2. FT-IR spectra of titanium dioxide–nylon–fluorophlogopite nanocomposite coating.

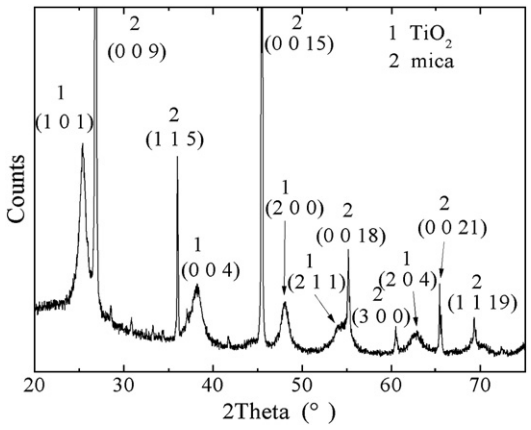

Fig. 4. XRD patterns of titanium dioxide–nylon 1010–fluorophlogopite nano composite coating sample (λ = 0.154 nm).

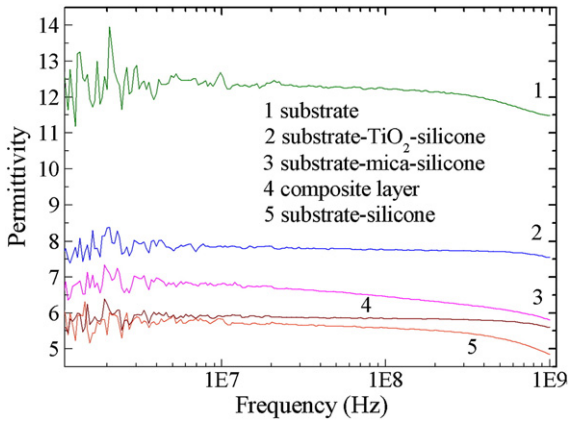

Fig. 5. Different dielectric constant of nano titanium dioxide–silicone–fluorophlogopite in different combinations to form composite layer.

After a binary composite coating with nano titanium dioxide, fluorophlogopite and silicone, the dielectric constant of silicone resin increased, but still comparatively decreased when contrasted with the substrate. There was a further drop of the dielectric constant attributed to the nano titanium dioxide–silicone–fluorophlogopite ternary composite coating compared to the binary composite coating coated substrate. The final preparation of the composite coating was ternary composite method.

4.4.2. Impedance measurement

Fig. 6 indicated a significant improvement in impedance when the cylinder was coated with a ternary titanium dioxide–silicone–fluorophlogopite. This coating not only reduced the dielectric constant, but also enhanced the real component (R) of high frequency impedance. The real part of complex impedance of substrate was about 20 Ω and the real part of complex impedance of nano titanium dioxide–silicone–fluorophlogopite ternary composite coating sample was about 32 Ω, increasing over 50%. This was mainly attributed to the addition of silicone resin, which leads to a significant increase in impedance. However, after adding nano titanium dioxide to the silicone resin, the real component R declined. This owes mainly to the semiconductor nature of titanium dioxide in a vacuum discharge flashover.

4.5. Nanosecond pulse vacuum insulation flashover performance test and result analysis

4.5.1. Experimental result

In these experiments, the standard nylon 1010 sample without nanocomposite coating was directly broken down, with a visible crack existing on surface. So nanosecond pulse vacuum flashover voltage of pure nylon 1010 without surface modification of nanocomposite coating was relatively low.

Each measurement of the sample show slight fluctuations with an increasing number of nanosecond pulse vacuum flashover discharges, accounting for the spread of experimental data in the nanosecond pulse vacuum flashover experiment as well as for the stability of the nanosecond square wave voltage pulse from Marx generator. Each sample took 20 times discharge and interval time of every discharge was 5 min. The breakdown voltage waveform of each discharge experiment was displayed on the oscilloscope. Taking into account data dispersivity of the experimental data and accuracy of nanosecond square wave voltage pulse from Marx generator, we make linear fitting by the least square method and exceptional obviously high or low flashover voltage was deleted. Flashover voltage was obtained by taking the average count from each result. The substrate in Fig. 7 was a standard nylon sample without any coating. The flashover voltage of the standard nylon 1010 sample was $12.55 \times 15.255 = 191.45$ kV. 15.25 k was attenuation coefficient taken from the electrode voltage of the vacuum chamber to oscilloscope display voltage number.

According to Fig. 7, flashover voltage increased to about 228.83 kV after adding silicone resin. Afterwards, the sample flashover voltage further increased to nearly 241.03 kV after adding nano titanium dioxide and fluorophlogopite respectively. Considering all these factors, we came to the conclusion that a final preparation of nanocomposite coating should use nano titanium dioxide, fluorophlogopite and organic silicone resin mixed in a mass ratio of 1:1:2.5. That led to flashover voltage of sample ultimately increasing to 252.47 kV. Nanosecond pulse vacuum flashover voltage thus gained a 31.87% increase over that of standard nylon after silicone–nano titanium dioxide–fluorophlogopite ternary nanocomposite coating on the nylon surface.

4.5.2. Analysis of flashover mechanism

When placed in a vacuum (10^{-3} Pa), gas desorption on insulator surface is necessary for the occurrence of high vacuum flashover. As surface solid molecules suffered an imbalanced attraction in all directions, a strong field formed. When gas molecules contacted with a solid surface, gas molecules fell into the range of forced field on the surface. The gas adsorption layer formed by adsorbed state can be attributed to the gas–solid adsorption bond [9].

If the applied voltage on both sides of the insulation was high enough, the cathode triple junction point engendered field electron emission. Surface adsorption gas would begin to desorb. That led to formation of an incentive gas channel between the cathode and anode. The incentive gas channel was the key to flashover development. Desorbed gas molecules absorbed electrons to become negative

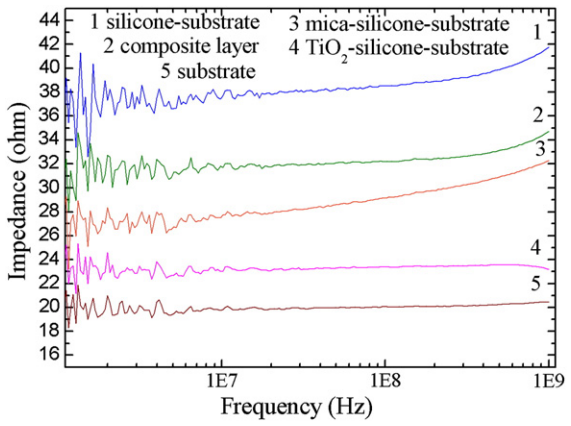

Fig. 6. High-frequency impedance of nano titanium dioxide–silicone–fluorophlogopite in different combinations to form composite layers.

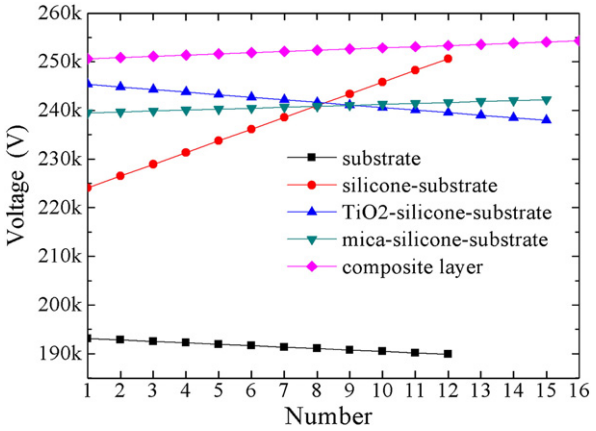

Fig. 7. Flashover voltage comparison chart of coating samples and standard sample of nylon.

ions, and desorbed gas may also be collided with electrons to make ionization happen. The charged gas molecules moved to the anode owing to the high voltage field and led to the formation of a secondary electron avalanche. Upon the formation of a neutral particle desorption channel along the surface, flashover occurred [10].

As a vacuum insulator, the insulativity of nylon 1010 was insufficient in the nanosecond pulse vacuum flashover experiment. Nylon 1010 cracked and decomposed from its surface, and carbonization was emerged on the brink of cracks, as shown in Fig. 8. A high magnification SEM image Fig. 8(b) shows there were a lot of amorphous carbon particles on the nylon 1010 surface crack section. In contrast, as shown in Fig. 1, samples with nano coating were not broken down in the experiment. The surface coating of sample was still intact after experiment.

4.5.3. Mechanism of flashover voltage improvement

In order to improve the flashover voltage of insulating material, there are two general ideas from the materials science vantage. 1) Pertaining to the composition of material, preparing materials of different composition. 2) Preparing new materials in some applications, although sometimes the conditions did not permit this. The only way to go by this was through material surface modification or coating. This is the basis of this study.

The efficacy of the surface coating treatment related to a variety of factors, such as coating materials, covering technology, insulation material substrate and its surface state under surface treatment, etc.. Since the role of insulator surface treatment is known, the modification effect mainly concerned the following: 1) decreasing the coefficient of secondary electron emission on insulator surface (which usually occurred near triple junction point, as shown in Fig. 9); 2) enhancing the surface non-conductibility; 3) reducing the insulator surface resistance coefficient; 4) reducing the degree of gas desorption on insulator surface; and 5) strengthening binding effect on substrate surface space charge.

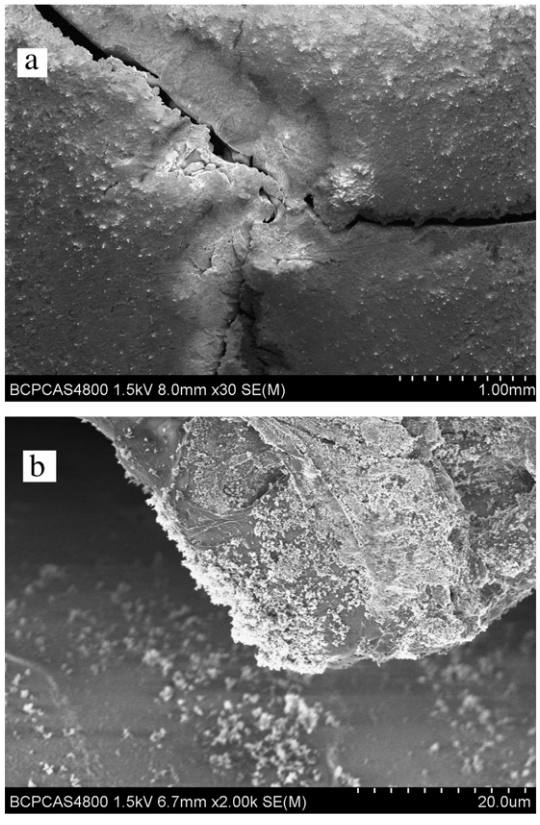

Fig. 8. SEM images of monolithic nylon 1010 after nanosecond pulse vacuum flashover experiment. (a) Broken down area. (b) Carbonization and cracks.

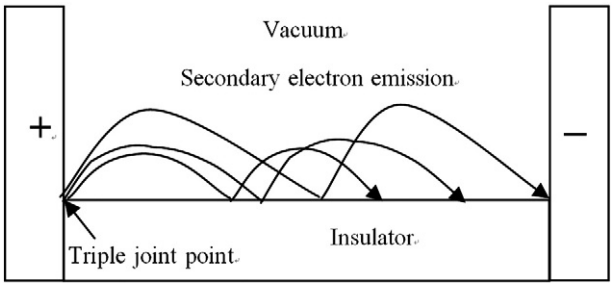

Fig. 9. Secondary electron emission from electrode–insulator–vacuum triple joint point.

The higher the relative dielectric constant of the material was; the worse insulation resistance in vacuum became. The reason was that the difference in the dielectric constant's influence on the potential line distribution near triple junction (vacuum, insulator, and electrode junction of the three). The higher the dielectric constant was, the greater the influence of electric field lines [15,16]. This leads to the electric potential lines near triple junction concentrate in the gap and field strength near triple junction increase dramatically.

As nano titanium dioxide powder and nylon 1010 were composited in nanocomposite method, nano titanium dioxide coated fluorophlogopite particles on surface. According to Figs. 2–4, a uniformly dispersed phase formed in the silicone and nylon 1010 substrate was completely covered by coating. The secondary electron emission coefficient of the nanosecond pulse discharge was greatly reduced due to large numbers of highly insulating organic silicon and fluorophlogopite.

The open circuit potential change of TiO_2 film with and without simulated solar light (about 3% ultraviolet light) radiation was shown in Fig. 10. TiO_2 films used in this experiment were fabricated on commercial Ti plates (99.99%) by micro-arc oxidation (MAO). All plates were cut into 20×20 (mm) samples which were used as working electrode. Influence of simulated solar light on the photogenerated voltage was performed to investigate photoelectric properties by electrochemical workstation (Zahner IM6e) with chronoamperometry. A 150 W metal halide lamp was used as an illuminate. This experiment shows the photoelectric response characteristics of titanium dioxide. When nano titanium dioxide film electrode worked as a photo-anode, the titanium plate's electrode potential shifted. When the titanium plate was under UV radiation, the potential dropped instantly.

Even gas desorbed on the surface generated an ionic charge. This charge should be taken away quickly to avoid accumulation because of titanium dioxide's photo-semiconductor property, thereby preventing material surface from flashover. As shown in Fig. 11, titanium dioxide was a good semiconductor under ultraviolet (UV) and visible light. It was composed of a low-energy valence band (filled with electrons) and a high-energy conduction band (empty with electrons). A photon whose energy was greater than or equal to the band gap could stimulate electrons in the valence band to migrate to the conduction band under light irradiation, forming an electron–hole pair. Surface charge can be rapidly eliminated by the electron–hole pair.

The reason why nano titanium dioxide doped in coating exhibited semiconductor property owes to the electroluminescence phenomena of the polyamide substrate associated with rising voltage from a high-voltage generator.

There was a very great difference between the surface molecule's structure and the internal molecule's structure within polyamide. Molecular chain breakage and folding, chemical bonding changes, molecular displacement caused by polarization, adsorption of gas molecules and other impurities existed on the surface of polyamide.

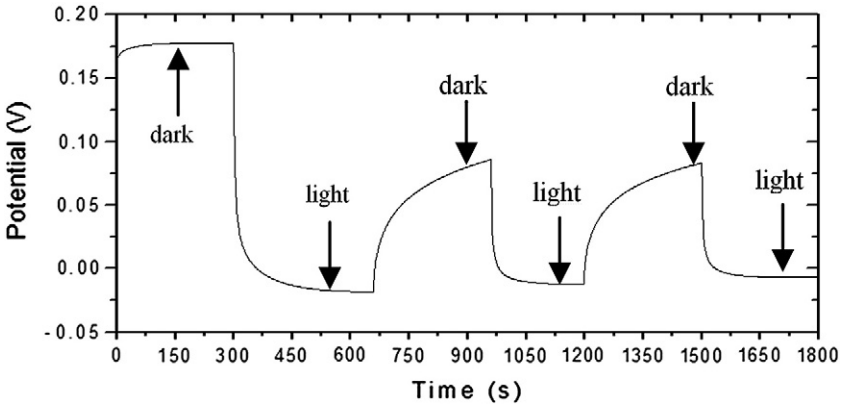

Fig. 10. Photoelectric corresponding curve of nano titanium dioxide.

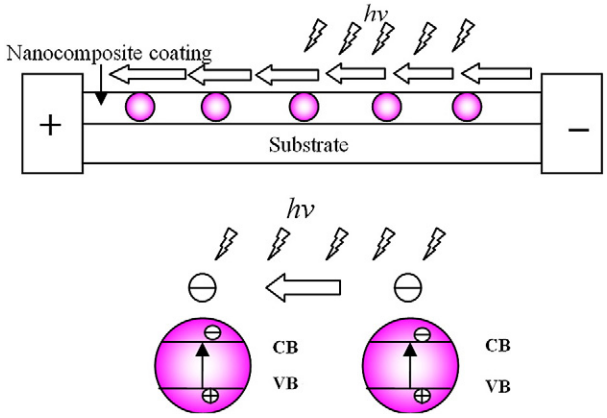

Fig. 11. Mechanism proposed for nano titanium dioxide photoelectric corresponding to UV radiation.

According to energy band theory, these phenomena will be ascribed to different energy levels which could be called surface state as a whole. The electron and hole in the electrode can be easily changed to surface state in discharge condition. Afterwards, these electrons and holes transferred within the polymer surface due to tunneling effect. When the electron and hole recombined, ultraviolet and visible light was produced [17].

Secondly, field emission occurred near cathode triple junction with increasing voltage. These electronics collided with surface molecules of polyamide and caused excitation and ionization of polyamide molecules and gas molecules adsorbed, resulting in strong ultraviolet light. The two above factors engendered the semiconductor property of nano titanium dioxide doped in coating.

In addition to the photoconductivity of titanium dioxide, covalent bond energies of titanium dioxide were stronger than polyamide substrate. The excitation and ionization of surface molecules became more difficult than that of polyamide, preventing flashover occurrence.

On the other hand, nanocomposite coating material used in this study decreased the dielectric constant, so that it affected the field strength on the triple junction less. It was also beneficial in improving the flashover voltage of the vacuum.

5. Conclusion

Nano titanium dioxide–silicone–fluorophlogopite nanocomposite coating on a surface imparts a low dielectric constant, high impedance, and semiconducting insulation properties. It also inhibits secondary electron emission under nanosecond pulsed flashover in vacuum. Adding titanium dioxide avoids formation and accumulation of surface charge owing to the photoconductivity of titanium dioxide. Hence, charge can be quickly transferred away. Nanocomposite coating also significantly reduces the dielectric constant of material, so the field strength on the triple junction was less affected. These specifications are beneficial to increasing the insulative properties of polyamide. Thus, the flashover voltage of polyamide coated by nanocomposite coating in vacuum is increased by 31% compared to that of neat polyamide and the high-voltage performance of organic insulators against flashover breakdown in vacuum is improved.

Acknowledgments

The work was financially supported by National Science Foundation of China under grant of NSAF10676018, 10776017 and 10876017. The authors are thankful to Institute of Electrical Engineering, Chinese Academy of Sciences (CAS) for performing flashover voltage measurement.

References

[1] X.M. Zhang, G. Li, D.M. Wang, Z.H. Yin, J.H. Yin, J.S. Li, Polym. 39 (1998) 15.
[2] M.L. Doche, V. Meynie, H. Mazille, C. Deramaix, P. Jacquot, Surf. Coat. Technol. 154 (2002) 113.
[3] C.H. De Tourreil, K.D. Srivastave, IEEE Trans. EI 8 (1973) 17.
[4] O. Yamamoto, T. Takuma, IEEE Trans. Electr. Insul. 10 (2003) 550.
[5] H. Craig Miller, IEEE Trans. Elect. Insul. 28 (1993) 512.
[6] H.D. Kim, H.G. Kim, J.J. Park, T.W. Kim, J.H. Kim, Proc. IEEE Intl. Conf. Properties Appl. Dielectric Mater. 2 (1997) 980.
[7] K. Hashimoto, H. Irie, A. Fujishima, Jpn. J. Appl. Phys. 44 (2005) 8269.
[8] L. Ying, L.S. Hon, T. White, R. Withers, L.B. Hai, Mater. Trans. 44 (2003) 1328.
[9] Y.Z. Li, S.J. Kim, J. Phys. Chem. B 109 (2005) 12309.
[10] Y.X. Zhang, G.H. Li, Y.C. Wu, Y.Y. Luo, L.D. Zhang, J. Phys. Chem. B 109 (2005) 5478.
[11] M. L. Kaplan, S. R. Forrest, P. H. Schmidt, T. Venkatesan, J. Appl. Phys. 55 (1984) 732.
[12] E.H. Lee, G.R. Rao, M.B. Lewis, L.K. Mansur, J. Mater. Res. 9 (1994) 1043.
[13] L.B. Bridwell, R.E. Giedd, Y.Q. Wang, S.S. Mohite, T. Jahnke, I.M. Brown, C.J. Bedell, C.J. Sotield, Nucl. Instr. Meth. B 56 (1991) 656.
[14] J.L. Zhu, Z.M. Lu, Z.W. Yu, Y.P. Guo, Z.T. Ma, R.Z. Beng, Nucl. Instr. Meth. B 91 (1994) 469.
[15] A.J. Dekker, Solid State Phys. 6 (1958) 251.
[16] O. Hachenberg, W. Brauer, in: L. Marton (Ed.), Advances in Electronics and Electron Physics, Academic Press, New York, 1959, p. 413.
[17] H. Seiler, J. Appl. Phys. 54 (1984) R1.
[18] L. Kelner, S.P. Markey, H.M. Fales, T.R. Lundquist, Int. J. Mass Spectrom. Ion Processes 62 (1984) 237.
[19] H. Boersch, H. Hamisch, W. Ehrlich, Zeitschr, J. Appl. Phys. 15 (1963) 518.
[20] A. Shih, J. Yater, C. Hor, R. Abrams, Appl. Surf. Sci. 111 (1997) 251.
[21] C.R. Li, T.S. Sudarshan, IEEE Trans. Dielectr. Electr. Insul. 2 (1995) 483.
[22] G.E. Hill, Vac. 26 (1976) 457.
[23] Junzo Ishikawa, Hiroshi Tsuji, Shigeo Ikeda, Yasuhito Gotoh, Nucl. Instrum. Meth. Phys. Res. Sect. B 12 (7) (1997) 282.
[24] K. Kimura, S. Usui, T. Tsujioka, S. Tanaka, K. Nakajima, M. Suzuki, Vac. 73 (1997) 59.
[25] A.J. Dekker, Advances in Research and Applications, Academic Press, New York, 1958, p. 251.
[26] A.S. Pillai, R. Hackam, J. Appl. Phys. 46 (1984) 1374.
[27] O. Milton, IEEE Trans. Electr. Insul. 7 (1972) 9.
[28] G. Maier, Prog. Polym. Sci. 26 (2001) 3.
[29] A. Sivathanu, R. Hackam, J. Appl. Phys. 58 (1985) 146.
[30] T. Mizuno, Y.S. Liu, W. Shionoya, K. Yasuoka, S. Ishii, H. Miyata, A. Yokoyama, IEEE Trans. Dielectr. Electr. Insul. 4 (1997) 433.